International Journal of Engineering Trends and Technology
ISSN: 2231 – 5381 / https://doi.org/10.14445/22315381/IJETT-V70I7P206
Volume 70 Issue 7, 49-59, July 2022

Original Article

Effect of Speed and Water Depth on Motion of Container Ship in Waves in Shallow Water

Tien Thua Nguyen[1], Thanh-Long Phan[2], Minh Tien Le[3]

[1,2,3]*Faculty of Transportation Mechanical Engineering, University of Science and Technology, The University of Danang, Danang City, Viet Nam.*

[1]ntthua@dut.udn.vn

Received: 25 May 2022 Revised: 30 June 2022 Accepted: 07 July 2022 Published: 18 July 2022

Abstract - *It is required to study the seakeeping performance to ensure a ship's safety and efficiency. The ship is not only operated on deep water journeys but also in shallow water during operation. In the deep sea, the characteristics of ships are mainly caused by random waves. However, the interaction between the ship and the bottom of the water usually occurs when the ship is moving in a shallow water area, and it can lead to change in the draft and motion of the ship as well as increasingly dangerous. This paper compares the motion characteristics of a container ship in harmonic waves in shallow waters with the ratios between the water depth and the ship's draft equal to h/T=1.2; 1.5; 2.0, and ∞. The ship responses varying with wave frequency are analyzed to evaluate the influence of shallow water on the ship's motion characteristics based on numerical simulation methods.*

Keywords - *Container ship, Effect of shallow water, Effect of ship speed, Ship motion characteristics, Regular waves.*

1. Introduction

A ship is not only designed to operate in the deep water region but also to move in the restricted area. Because ship size has increased to meet the demand for cargo transport, ship motion in shallow water has become more attractive to the scientific community. In the deep water case, the seakeeping of the ship concentrates on the ship's response to waves in infinite water depth. However, ship motion in shallow water considers the ship behaviors under the interaction between the hull and seabed that may be led to trim, sinking, and squat phenomena. Hence, IMO (International Maritime Organization) recommended that the ship motion characteristics in shallow water conditions should be included in IMO A.601 [1].

When the ship is moving in shallow water, the flow velocity is accelerated as it passes through the gap between the bottom of the ship and the bottom of the water area. According to Bernoulli's principle, the pressure field in that area is reduced, causing the ship to be sunk and trimmed and reducing buoyancy. These phenomena cause changes in transverse flow forces and inertia and lift forces [2]. Therefore, the hydrodynamic forces and moments acting on the hull are also changed, resulting in variations in the ship's motion in waves. Several studies have conducted ship maneuvering behavior in shallow water [3-11].

On the other hand, seakeeping performance is an important characteristic that enables a ship to operate safely and efficiently. Some authors have studied the influence of the water bottom on this characteristic [12-16]. One of the first studies of ship motion on waves in shallow water was done by Vantorre et al. [12]. In this study, the author experimented to determine the heaving and swaying motion of the ship on harmonic waves and investigated the influence of speed on sinkage. The results are then used to calculate the collision probability with the water area's bottom.

Following this, Ruiz et al. investigated the influence of shallow water on the 6-degrees-of-freedom motion of the KVLCC2 model in shallow water [2]. The results show that the ship motion response reaches the maximum value in the case of ocean waves with a length of approximately 1/3 of the ship's length. The mean drift force acting on the hull is also determined in this study. In addition, the DTC container ship in waves in shallow water was carried out at two ratios between draft and water depth of 20% and 100% by Zwijnsvoorde [17]. The results of heave, roll, and pitch motions were investigated by uncertainty analysis.

This study investigates the seakeeping of a container ship at various speeds and different shallow water conditions. The potential-based Rankine panel method simulates a full-scale model in regular waves for estimating

the ship motion responses, steady drift wave force, and the moment [18-23]. The ship's heave, roll, and pitch motion in very shallow water in waves are verified with experimental data. Finally, the effects of speeds and shallow water conditions on the ship's motion characteristics are analyzed.

2. Theory Background

2.1. Fundamentals of Ship Motion in Waves

Two coordinate systems are adopted for investigating the ship's motion in waves. The body-fixed frame, $Gx_by_bz_b$, is attached to the hull so that Gx_b, Gy_b, and Gz_b are the longitudinal axis in the forward direction of the ship, the transverse axis to the port side of the ship, and the vertical axis directed upwards. G stands for the ship's center of gravity. The global coordinate frame, *OXYZ*, is located in the universe domain in which the origin O lies on the mean free surface of the liquid. The *Z*-axis is directed vertically upwards, and the *Y*-axis is directed to the left. The ship motion components include three translational motions along the x_b-axis, y_b-axis, and z_b-axis, and three rotational motion components about the axes are illustrated in Figure 1. The motion components of the ship are defined as follows:

$$\vec{X} = [x \quad y \quad z \quad \phi \quad \theta \quad \psi]^T \tag{1}$$

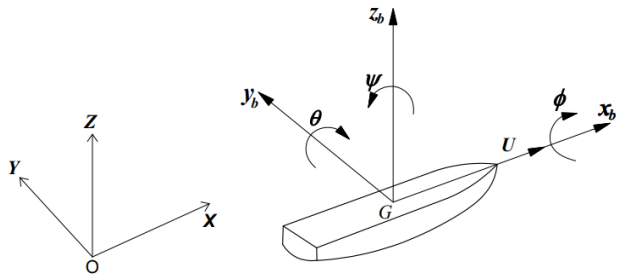

Fig. 1 Coordinate systems and symbol

$$\sum_{k=1}^{6}\left[\left(M_{jk}+A_{jk}\right)\ddot{X}+B_{jk}\dot{X}+C_{jk}X\right]=F_j e^{i\omega t}; j=1\div 6 \tag{1}$$

Where M_{jk}, A_{jk}, B_{jk}, and C_{jk} are mass of the ship, added mass, damping, and restoring force, respectively. F_j and ω are the external forces and frequency of incident waves [24].

Potential flow is often opted for simulating the seakeeping performance of a ship because of its efficiency in time and accuracy. Governing equations and boundary conditions of the method are described as follows [25]:

+ Laplace equation in fluid domain Ω:

$$\frac{\partial^2\varphi}{\partial x^2}+\frac{\partial^2\varphi}{\partial y^2}+\frac{\partial^2\varphi}{\partial z^2}=0 \tag{2}$$

+ Boundary conditions on the free water surface and body surface area:

$$(-i\omega_e+\vec{U}.\nabla)^2\varphi+g\frac{\partial\varphi}{\partial z}=0 \tag{3}$$

$$\frac{\partial\varphi_r}{\partial n}=-i\omega_e n_j+Um_j\ ;\frac{\partial\varphi_d}{\partial n}=-\frac{-\partial\varphi_I}{\partial n} \tag{4}$$

where

$$(m_1,m_2,m_3)=(0,0,0),\ (m_4,m_5,m_6)=-\frac{1}{U}\vec{U}\times\vec{n}$$

+ On the bottom of the water area:

$$\frac{\partial\varphi}{\partial z}=0 \tag{5}$$

+ Potential velocity becomes zero at the farfield area.

Considering fluid flow around the hull, potential velocity consists of three components incident wave φ_I, diffracted wave φ_D, and radiation wave φ_{rj}, such as:

$$\left.\begin{aligned}\Phi(\vec{X},t)&=A\varphi\left(\vec{X}\right)e^{-i\omega_e t}\\ \varphi\left(\vec{X}\right)e^{-i\omega_e t}&=\left[(\varphi_I+\varphi_d)+\textstyle\sum_{j=1}^{6}\varphi_{rj}.x_j\right]e^{-i\omega_e t}\end{aligned}\right\} \tag{6}$$

The potential velocities of diffraction and radiation waves can be determined from the Green function. The first-order hydrodynamic pressure, *p*, is then determined through the Bernoulli equation. The wave force F_{lj}, diffracting force F_{dj}, and radiation force F_{rjk} are obtained as follows:

$$p=\rho\left[i\omega_e\varphi(\vec{x})+\vec{U}.\nabla\varphi(\vec{x})\right]e^{-i\omega_e t} \tag{7}$$

$$F_{Ij}=-\rho\int_{S_0}\left\{(i\omega_e+\vec{U}.\nabla)\varphi_I(\vec{x})\right\}n_j dS \tag{8}$$

$$F_{dj}=-\rho\int_{S_0}\left\{(i\omega_e+\vec{U}.\nabla)\varphi_d(\vec{x})\right\}n_j dS \tag{9}$$

$$F_{rjk}=-i\omega_e\rho\int_{S_0}(n_j+\frac{i}{\omega_e}\vec{U}.\nabla n_j)\varphi_{rk}(\vec{x})\,dS \tag{10}$$

Where S_0 is the mean wetted surface of the ship.

Finally, the ship response in the frequency domain can be achieved by solving the following equation,

$$\left[x_{jm}\right]=H\left[F_j\right] \tag{11}$$

$$H=\left\{-\omega_e^2\left(M_{jk}+A_{jk}\right)-i\omega_e B_{jk}+C_{jk}\right\}^{-1} \tag{12}$$

2.2. Mean Drift Force Acting on Ship

The second-order wave can be computed from the quadratic products of quantities derived from the linear wave theory. The wave's exciting force and moment on the ship's hull can be determined according to

$$\vec{F}^{(2)} = -\frac{1}{2}\rho g \oint_{WL} \zeta^{(1)} \cdot \zeta^{(1)} \vec{n} dl + \frac{1}{2}\rho \iint_{S_0} \left[\nabla \Phi^{(1)} \cdot \nabla \Phi^{(1)}\right] \vec{n} dS + \rho \iint_{S_0} \left[\vec{X}^{(1)} \cdot \nabla \frac{\partial \Phi^{(1)}}{\partial t}\right] \vec{n} dS + \vec{\alpha}^{(1)} \times \vec{F}^{(1)} + \rho \iint_{S_0} \frac{\partial \Phi^{(2)}}{\partial t} \vec{n} dS \quad (13)$$

$$\vec{M}^{(2)} = -\frac{1}{2}\rho g \oint_{WL} \zeta^{(1)} \cdot \zeta^{(1)} (\vec{X} \times \vec{n}) dl + \frac{1}{2}\rho \iint_{S_0} \left[\nabla \Phi^{(1)} \cdot \nabla \Phi^{(1)}\right] (\vec{X} \times \vec{n}) dS + \vec{\alpha}^{(1)} \times \vec{M}^{(1)} + \rho \iint_{S_0} \left[\vec{X}^{(1)} \cdot \nabla \frac{\partial \Phi^{(1)}}{\partial t}\right] (\vec{X} \times \vec{n}) dS + \rho \iint_{S_0} \frac{\partial \Phi^{(2)}}{\partial t} (\vec{X} \times \vec{n}) dS \quad (14)$$

The second order wave exciting force and moment due to the first order waves and motion responses resulting from a pair of the regular incident waves with (a_{jm}, ω_{jm}, χ_m, α_{jm}) and (a_{kn}, ω_{kn}, χ_n, α_{kn}) can be written as

$$\vec{F}_{jkmn}^{(2)} = a_{jm} a_{kn} \{\vec{P}_{jkmn}^{+} \cos[(\omega_{jm} + \omega_{kn})t - (\alpha_{jm} - \alpha_{kn})] + \vec{Q}_{jkmn}^{+} \sin[(\omega_{jm} + \omega_{kn})t - (\alpha_{jm} - \alpha_{kn})] + \vec{P}_{jkmn}^{-} \sin[(\omega_{jm} + \omega_{kn})t - (\alpha_{jm} - \alpha_{kn})] + \vec{Q}_{jkmn}^{-} \sin[(\omega_{jm} + \omega_{kn})t - (\alpha_{jm} - \alpha_{kn})]\} \quad (15)$$

where $\vec{P}_{jkmn}^{+}$ and $\vec{Q}_{jkmn}^{+}$ are called the sum of frequency force components, while $\vec{P}_{jkmn}^{-}$ and $\vec{Q}_{jkmn}^{-}$ Contribute only to the difference frequency force components.

In this study, mean wave drift force and moment acting on the ship in all motion directions are calculated based on the wetted surface integration approach. The sum frequency force components are excluded. The mean wave drift force of the long-crested wave of individual direction is defined as:

$$\overline{\vec{F}^{(2)}} = \sum_{j=1}^{N_w} a_{j1}^2 \vec{P}_{jj11}^{-} \quad (16)$$

The respective normalized coefficients of the mean drift forces and moment are defined as follows:

$$C_x = \frac{-\overrightarrow{F_x}^{(2)}}{\rho g A^2 (B^2/L)}, \; C_y = \frac{\overrightarrow{F_y}^{(2)}}{\rho g A^2 (B^2/L)}, \; C_N = \frac{\overrightarrow{M_z}^{(2)}}{\rho g A^2 B^2} \quad (18)$$

3. Numerical Simulation

3.1. Case study

In this research, the KRISO Container Ship (KCS) model is used to evaluate motion characteristics in water waves in shallow water for various ship speeds and different water depths. The seabed is considered a plane, and the bank effect does not exist. The main parameters of the KCS model are presented in Table 1 [26].

Table 1. Main parameters of the KCS model

Item	Value	Unit
Length between perpendiculars, L_{PP}	230	m
Breadth, B	32.2	m
Draft, T	10.8	m
Longitudinal center of gravity, LCG	111.6	m
The vertical center of gravity, KG	10.8	m
Radius of gyration, (k_{xx}, k_{yy}, k_{zz})	(0.4B, 0.25L, 0.25L)	m

Figure 2 depicts the definition of wave direction and velocity of a ship in the coordinate system fixed to the hull. The wave direction is defined based on the relative position between the wave and the ship. The wave frequency is selected based on the Pierson-Moskowitz wave spectrum, where the wave energy has a significant value and is suitable for the operating conditions of the ship in shallow water. The wave frequency range from 0.2 to 1.2 rad/s is selected in this case.

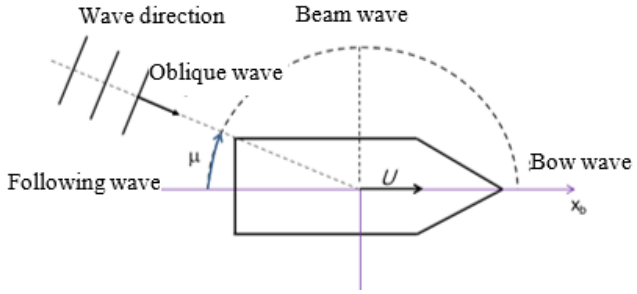

Fig. 2 Definition of wave direction

3.2. Numerical modeling

The ship's motion in waves in shallow water is simulated based on the boundary element analysis in Ansys AQWA 19.2 software. Following this method, the computational model is discretized into 35454 elements, including 16541 diffracted elements. Fig. 3 shows the KCS ship model approximated by the grid elements. Furthermore, ship speed, wave frequency, and depth of water area are defined for evaluating the influence of ship speeds and water depths on the ship's performance in various wave frequencies.

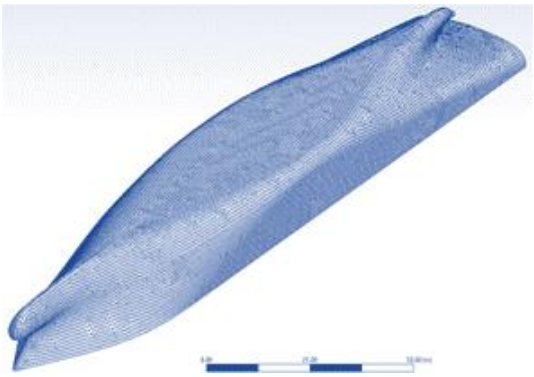

Fig. 3 Generated meshing on the KCS model

4. Results and Discussion

4.1. Verification Study

KCS motion in shallow water in regular waves is analyzed using the boundary element approach in Ansys Aqwa 19.2. The obtained results are compared with experimental and simulation results based on the strip theory method [2]. It can be seen that the heave and pitch motion of the model are quite similar to the experimental data. However, the calculation results from strip theory are much different from the others, as shown in Figure 4a and Figure 4b. On the other hand, the ship's roll motion in the case of the following wave is also compared with the experimental and theoretical results in Figure 4c. In this case, the boundary element method gives smaller results than the experimental ones, while the strip theory method gives more similar results than experimental data. Based on this comparison, the ship motion characteristics in a head sea, oblique bow sea, and beam sea in shallow water will be analyzed in the next section.

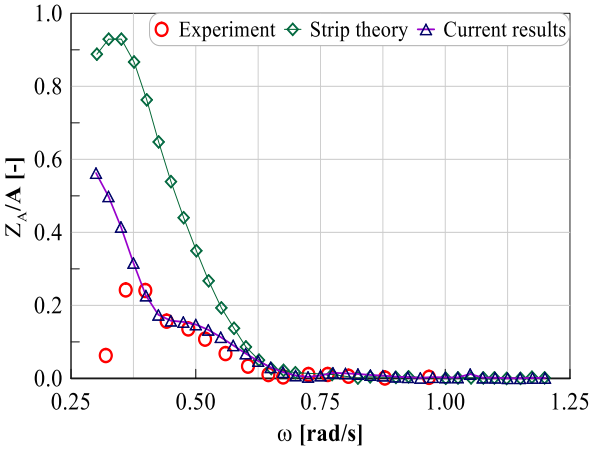

a) Heave motion versus frequency, μ=180°

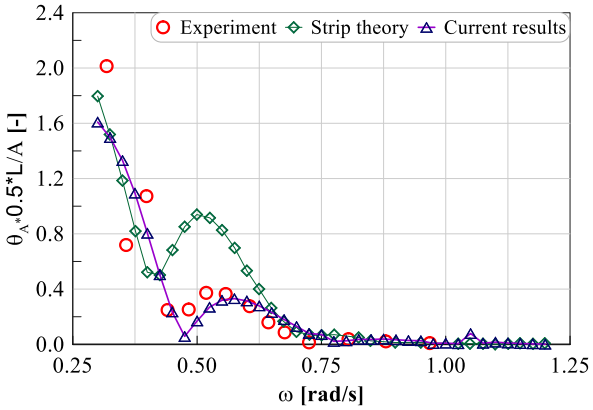

b) Pitch motion versus frequency, μ=180°

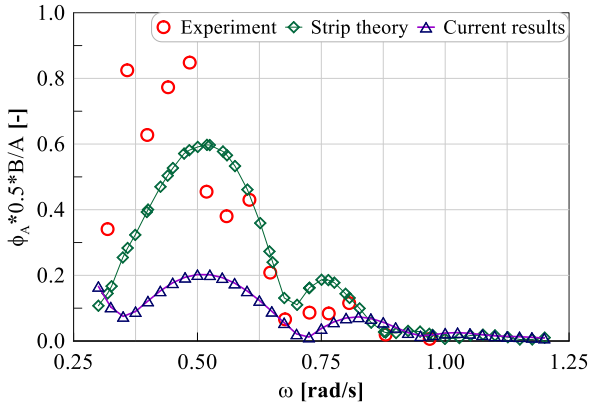

c) Roll motion versus frequency, μ=10°

Fig. 4 Comparison of heave, roll and pitch motion of KCS model in the head sea at V=12Knots and h/T=1.2

4.2. Effect of Speed on Ship Response in Shallow Water

The motion responses of the KCS container ship in harmonic waves at different speeds V_1=5.0knots, V_2=7.0knots, and V_3=9.0knots are calculated. The boundary element approach is used to simulate the motion of ships in regular waves conditions. The influence of the speed on ship motion in very shallow water at different wave directions is depicted in Fig. 5. The results show that the heave, roll, and pitch motions increase as the ship performs in long waves. However, the ship responses in short waves become smaller than in deep water cases. The left motion components are less affected by the change in the shipping speed.

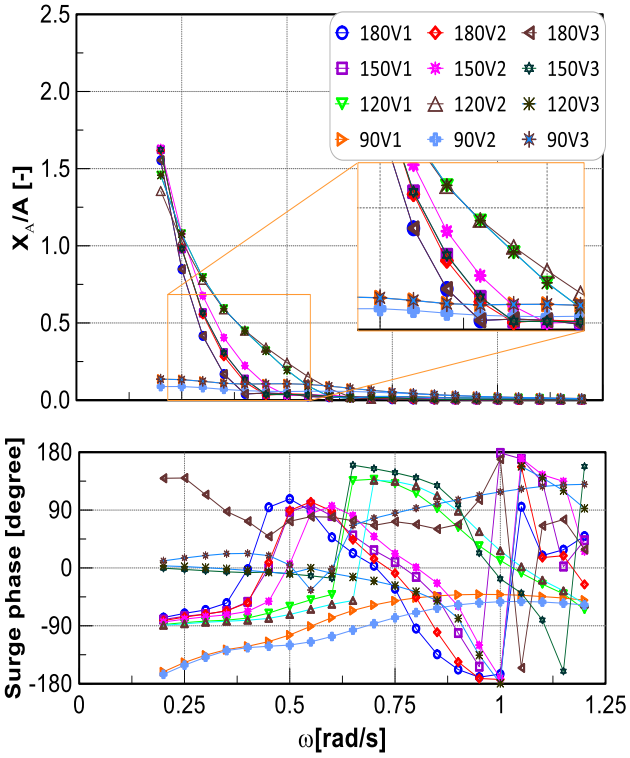

a) Surge motion

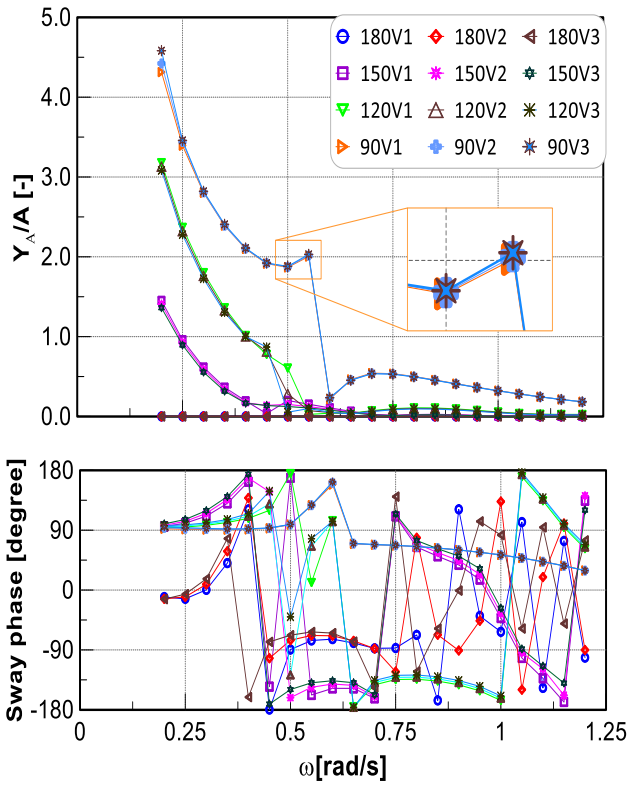

b) Sway motion

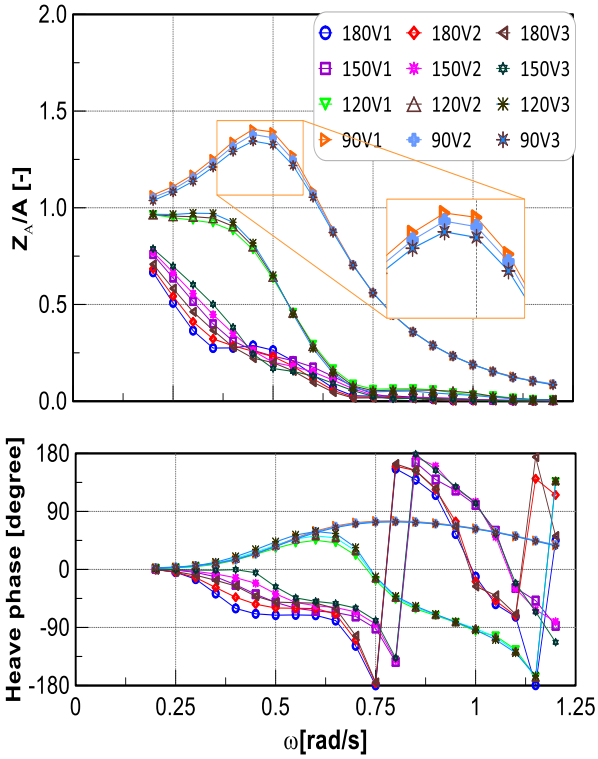

c) Heave motion

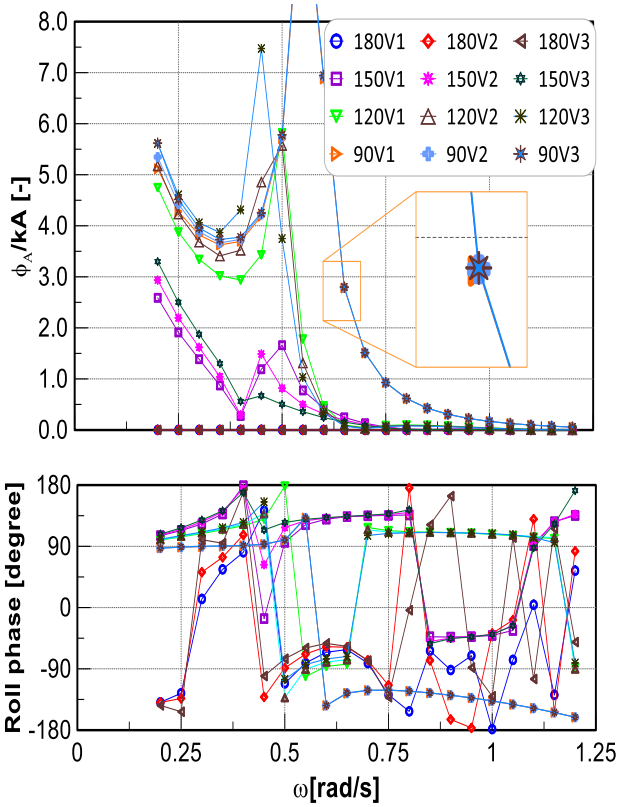

d) Roll motion

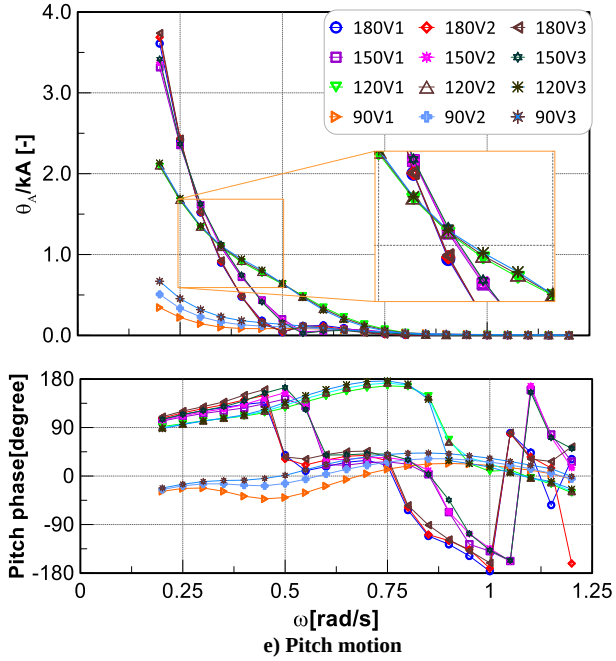

e) Pitch motion

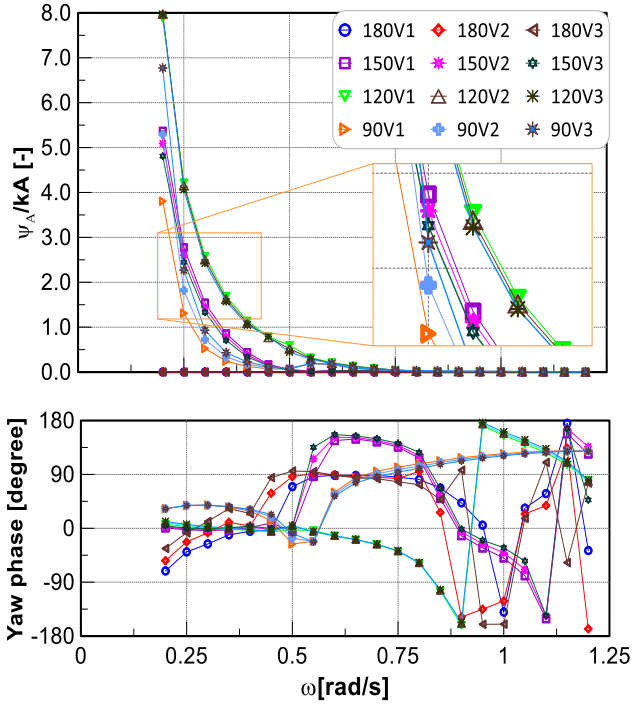

f) Yaw motion

Fig. 5 Motion characteristics of KCS model at various speeds and water depth ratio of 1.2

4.3. Effect of Water Depth on Ship Response

The effects of shallow water conditions on the seakeeping performance of the KCS model at a speed of 7.0 knots are presented in Fig. 6. It has shown that the ship responses in long waves have increased significantly as the water depth decreased. When the wavelength decreases, the ship motion components are smaller than the corresponding motions in deeper water. It can be explained by the fact that long waves have much greater energy than in the case of short waves. The translational motion in the x-direction is significantly increased in the case of diagonal waves. Meanwhile, translational motion in the y-direction reaches a local maximum when the ship passes through transverse or diagonal waves. It can be interpreted by the flow velocity increase when passing through the narrow gap between the ship and the bottom of the water area. Consequently, a large difference in pressure and draft between the two sides of the ship appears. The influence of shallow water on the heave motion is clearly shown when the ship moves on beam waves. This motion component increases as the water depth and draft ratio decrease, as shown in Figure 6c. Similarly, the effect of water depth on the roll motion is also greatest when the angle between the wave and the hull is 90°. However, the results of this motion component do not consider the effect of fluid viscosity. The pitch motion is greatly increased in the case of head sea and oblique waves, Figure 6e. This motion component increases most when the ship moves over the heat wave in a shallow water area. Ship yaw motion is most enhanced by the decrease in water depth in oblique waves, as shown in Figure 6f.

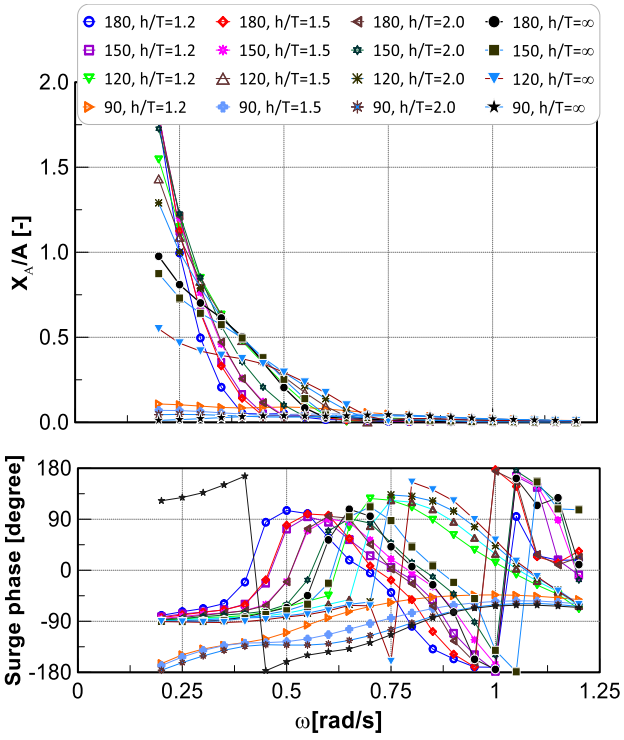

a) Surge motion

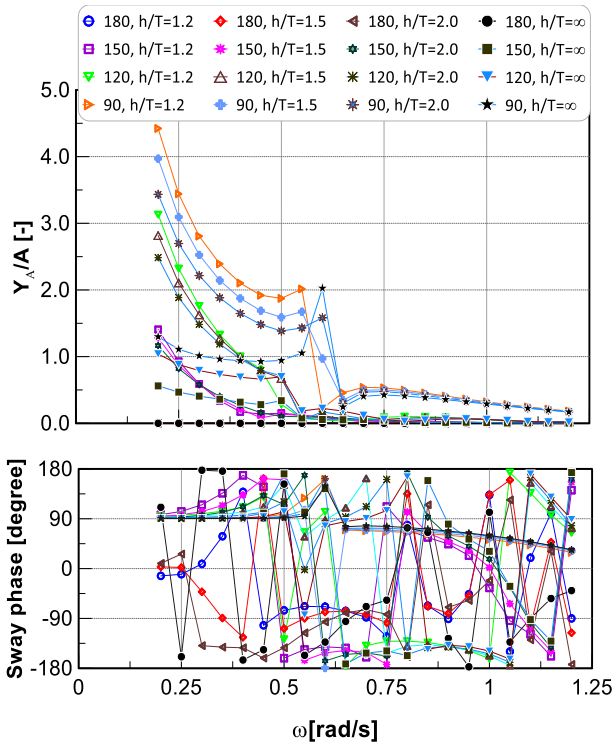

b) Sway motion

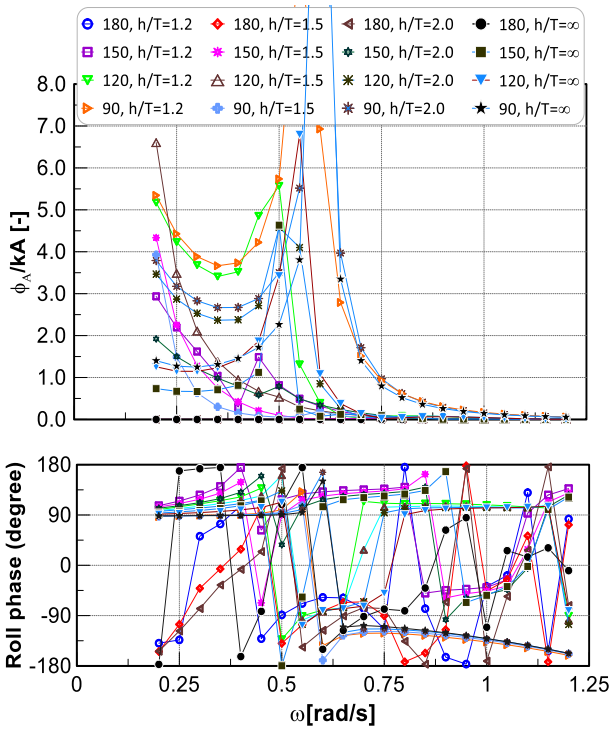

d) Roll motion

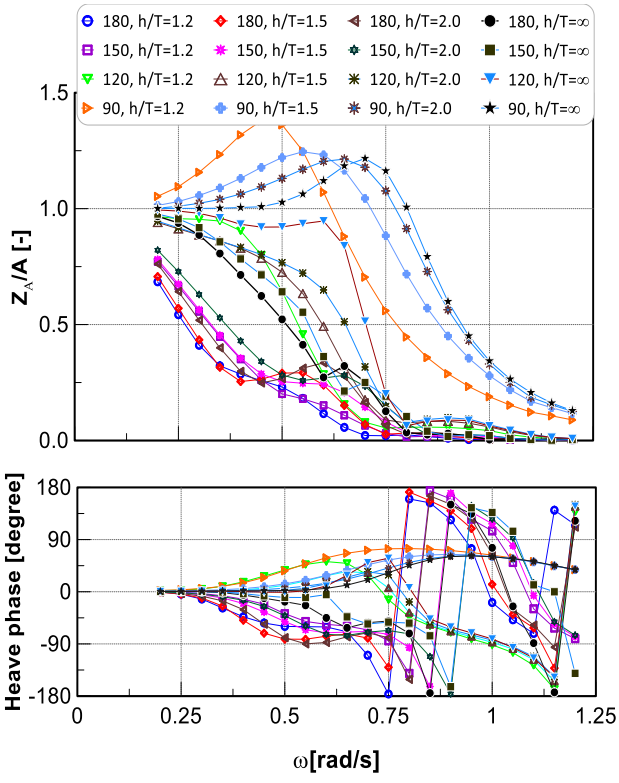

c) Heave motion

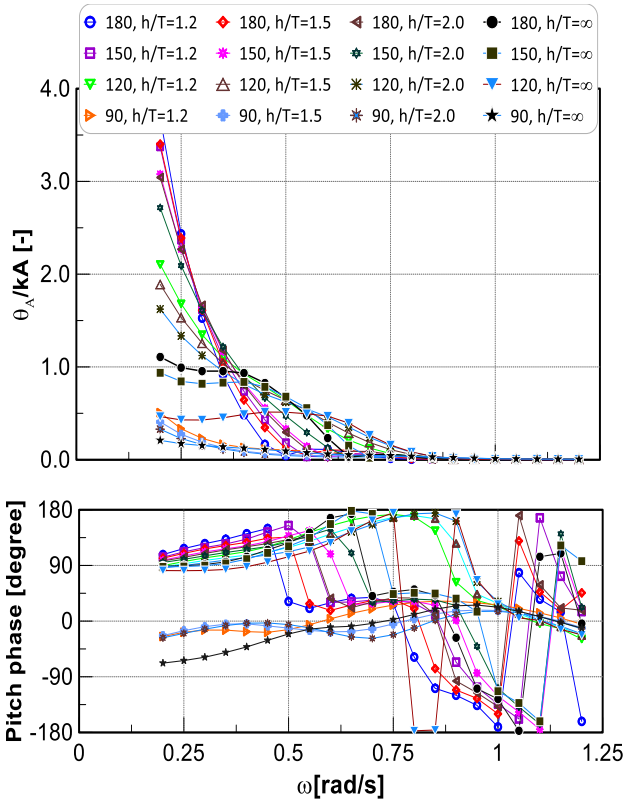

e) Pitch motion

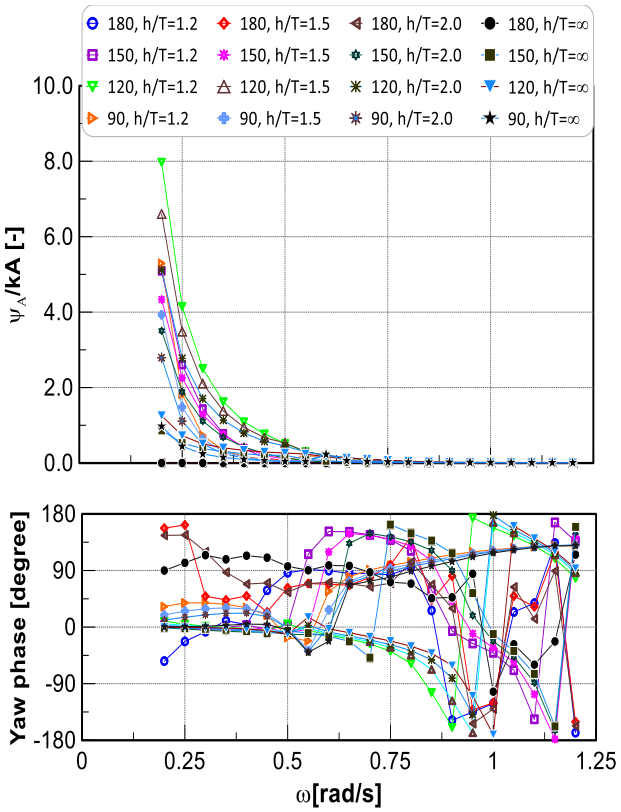

f) Yaw motion

Fig. 6 Motion characteristics of KCS model at different water depth ratios and speed of 7.0 knots

4.4. Effect of Water Depth on Steady Drift Forces

The previous sections introduce the formulation of the mean drift wave force on a ship. The normalized coefficients of the longitudinal, transverse, and yaw moment at a ship speed of 7.0 knots as a function of water depth for a set of wave frequencies are shown in Fig. 7-9. It can be seen that the mean drift forces of the KCS model are significantly increased when the water depth is decreased. Under the head sea condition, the surge drift force becomes the largest at the frequency of 0.625 rad/s. A similar trend has been observed from the transverse force. The force has reached maximum value as the ship is in beam sea condition. The overall trends are also similar for yaw moment coefficients, but there are significant discrepancies in yaw drift moment at the wave directions of 120 and 150 degrees. The coefficient reaches a peak value as the ship moves in beam sea waves.

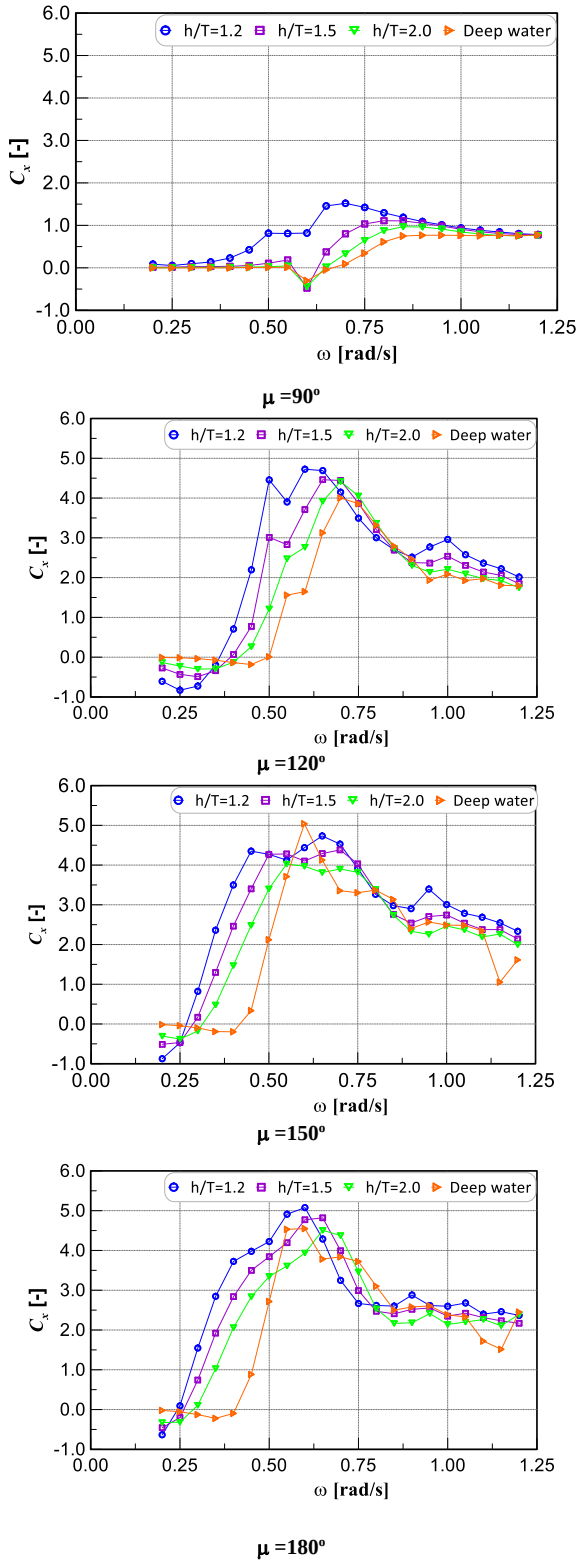

Fig. 7 Steady longitudinal force coefficients of KCS model at various wave directions and ship speed of 7.0 knots

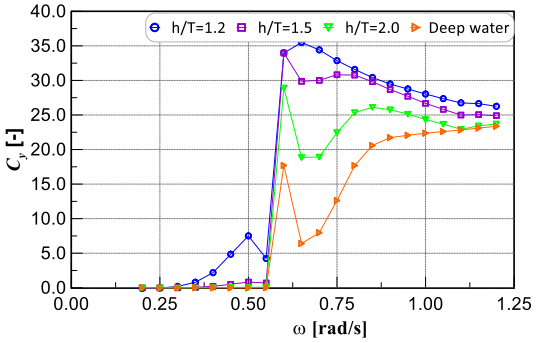

μ =90°

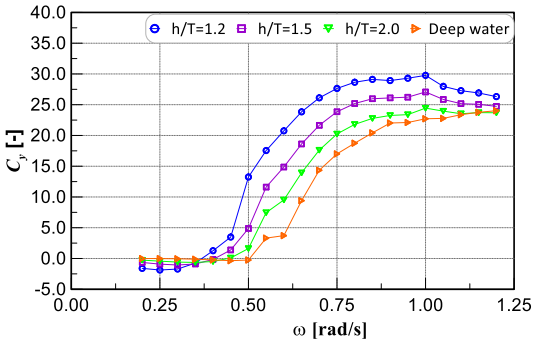

μ =120°

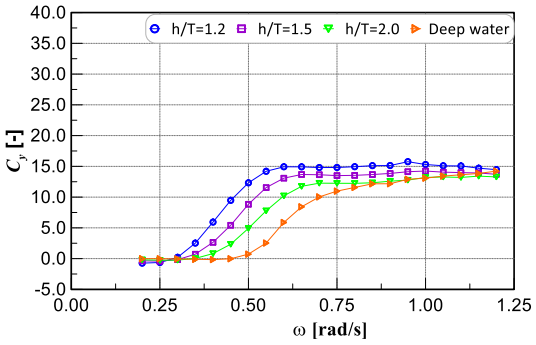

μ =150°

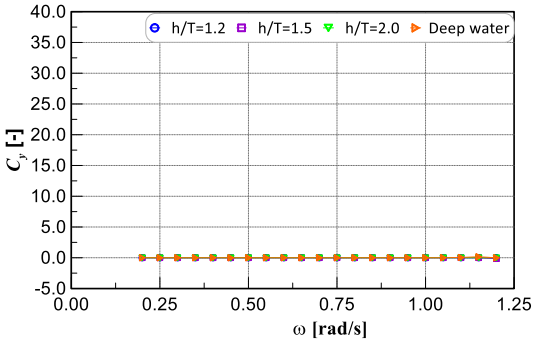

μ =180°

Fig. 8 Steady transverse force coefficients of KCS model at various wave directions and ship speed of 7.0 knots

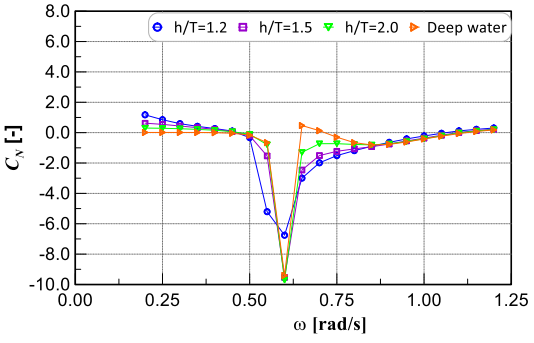

μ = 90°

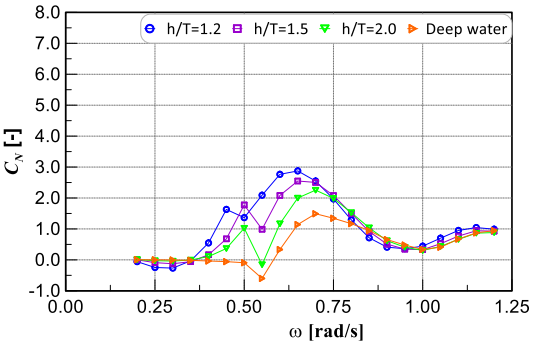

μ = 120°

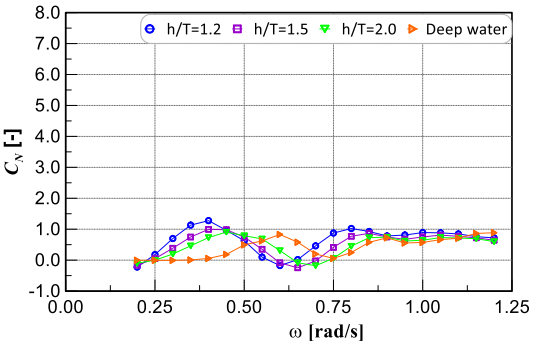

μ = 150°

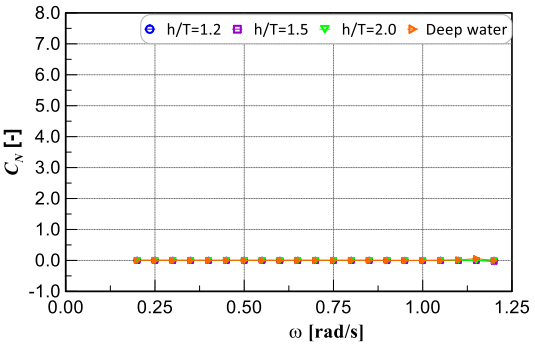

μ = 180°

Fig. 9 Steady yaw moment coefficients of KCS model at various wave directions and ship speed of 7.0 knots

5. Conclusion

The motion of the container ship on harmonic waves in shallow water was analyzed based on the boundary element approach at various speeds and different water depths. Some conclusions are drawn as follows:

- The ship's speed considerably affects the ship's motion in long waves. As wavelength decreases, the ship responses in deep water are larger than the corresponding motion in shallow water. The effect of speed on ship motion in small wavelengths is negligible.

- Water depth has a great influence on the movement of ships in long waves. The heave motion has increased most when moving in a beam sea. As wavelength decreases, the ship motion components in deep water tend to be larger than the corresponding motion in shallow water. Pitch motion reaches a maximum when the ship moves against the waves.

- The roll motion resonance phenomenon occurs in the beam sea case. However, the maximum value of this motion is not accurate because it ignores the influence of viscous force.

- The mean drift forces and moment are significantly enlarged when the ship operates in shallow water. The surge drift force reaches the maximum when the ship runs in head sea condition. The sway drift force and yaw moment get the peak values in beam and oblique sea cases of 120 degrees, respectively.

Funding Statement

Funds fund this research for Science and Technology Development of the University of Danang under project number: [B2019-DN02-63].

References

[1] "Provision and Display of Manoeuvring Formation on Board Ships," *IMO Resolution A*, vol. 601, no. 15.

[2] M.T. Ruiz, S. D. Caluwé, T.V. Zwijnsvooorde, G. Delefortrie, M. Vantorre, "Wave Effects in 6DOF on a Ship in Shallow Water,"*in Proc. MARSIM 2015*, pp.8-11, 2015.

[3] Akhil Balagopalan, P. Krishnankutty, "Manoeuvring Prediction of a Container Ship in Shallow Water Using Numerical Planar Motion Mechanism," *Ship Technology Research*, vol. 68, no. 3, pp. 147-165, 2021.

[4] C. Chen, G. Delefortrie, E, Lataire, "Effects of Water Depth and Speed on Ship Motion Control from Medium Deep to Very Shallow Water," *Ocean Engineering*, vol. 231, pp. 102-109, 2021.

[5] S.H. Kim, C.K. Lee, Y.B. Chae, "Prediction of Maneuverability in Shallow Water of Fishing Trawler by Using Empirical Formula," *J Mar Sci Eng.*, vol. 9, pp. 1392, 2021.

[6] J. Hooft, "Manœuvring Large Ships in Shallow Water—I," *Journal of Navigation*, vol. 26, no. 2, pp. 189-201, 1973.

[7] K. Eloot, G. Delefortrie, M. Vantorre, F. Quadvlieg, "Validation of Ship Manoeuvring in Shallow Water through Free-Running tests," *in Proc. OMAE2015*, pp. 1–11, 2015.

[8] M.T. Ruiz, M. Mansuy, G. Delefortrie, "Manoeuvring Study of a Container Ship in Shallow Water Waves," *in Proc.OMAE2018*, pp. 1-10, 2018.

[9] Haitong Xu, C. Guedes Soares, "Hydrodynamic Coefficient Estimation for Ship Manoeuvring in Shallow Water Using an Optimal Truncated LS-SVM," *Ocean Engineering*, vol. 191, pp. 1-13, 2019.

[10] P. Krishnankutty, A. Kulshrestha, "Estimating Manoeuvring Coefficients of a Container Ship in Shallow Water Using CFD," *in Proc.MARHY*, pp. 285-292, 2014.

[11] K. Atreyapurapu, B. Tallapragada, K. Voonna, "Simulation of a Free Surface Flow over a Container Vessel Using CFD," *International Journal of Engineering Trends and Technology*, vol. 18, no. 7, pp. 334-339, 2014.

[12] M. Vantorre, L. Erik, K. Eloot, J. Richter, J. Verwilligen, E. Lataire, "Ship Motions in Shallow Water as the Base for a Probabilistic Approach Policy," *in Proc. 27th ASME*, pp. 349-358, 2008.

[13] T. Tezgogan, A. Incecik, O. Turan, "Full-scale unsteady RANS Simulations of Vertical Ship Motions in Shallow Water," *Ocean Engineering*, vol. 123, no. 1, pp. 131-145, 2016.

[14] M. Naciri, N. Southall, "Seakeeping of a Non-Wall Sided Vessel in Shallow Water: Lessons Learnt From Experiments and Numerical Analyses," *in Proc. OMAE2007*, pp. 535-543, 2007.

[15] W. Zhang, O. Moctar, T.E. Schellin, "Numerical Study on Wave-Induced Motions and Steady Wave Drift Forces for Ships in Oblique Waves," *Ocean Engineering*, vol. 196, pp. 1-13, 2020.

[16] C.B. Yao, X.S. Sun, W. Wang, Q. Ye, "Numerical and Experimental Study on Seakeeping Performance of Ship in Finite Water Depth," *Applied Ocean Research*, vol. 67, pp. 59-77, 2017.

[17] T.V. Zwijnsvoorde, T.V. Ruiz, M.T. Ruiz, G. Delefortrie, E. Lataire, "Sailing in Shallow Water Waves with the DTC Container Carrier: Open Model Test Data for Validation Purposes," *in Proc. 5th MASHCON*, pp. 19-23, 2019.

[18] A. von Graefe, "Rankine Source Method for Seakeeping Analysis in Shallow Water," *in Proc. OMAE2014*, pp. 211-219, 2014.

[19] C.B. Yao, X.S. Sun, W.M. Liu, D.K. Feng, "Seakeeping Computation of Two Parallel Ships with Rankine Source Panel Method in Frequency Domain," *Engineering Analysis with Boundary Elements*, vol. 109, pp. 70-80, 2019.

[20] Md. Shahjada. Tarafder, K. Suzuki, "Wave-Making Resistance of a Catamaran Hull in Shallow Water Using a Potential-Based Panel Method," *J Ship Res*, vol. 52, pp. 16-29, 2008.

[21] E. Yasuda, H.Iwashita, M. Kashiwagi, "Improvement of Rankine Panel Method for Seakeeping Prediction of a Ship in Low Frequency Region," *in Proc. OMAE2016*, pp. 163-171, 2016.

[22] P. Zhang, T. Zhang, X. Wang, "Hydrodynamic Analysis and Motions of Ship with Forward Speed via a Three-Dimensional Time-Domain Panel Method," *J Mar Sci Eng*, vol. 9, no. 1, pp. 87-105, 2021.

[23] F. Pacuraru, L. Domnisoru, S. Pacuraru, "On the Comparative Seakeeping Analysis of the Full Scale KCS by Several Hydrodynamic Approaches," *J Mar Sci Eng*, vol. 8, no. 12, pp. 962-993, 2020.

[24] Edward. V. Lewis, "Principles of Naval Architecture: Volume III – Motion in Waves," 1st ed., *Society of Naval Architects and Marine Engineers (SNAME)*, pp. 41-42, 1988.

[25] H. Chanson, "Applied Hydrodynamics: An Introduction to Ideal and Real Fluid Flows," 1st ed., *CRC Press, Taylor & Francis Group*, pp. 29-136, 2009.

[26] W. J. Kim, D. H. Van, and D. H. Kim, "Measurement of Flows Around Modern Commercial Ship Models," *Exp. in Fluids*, vol. 31, pp. 567-578, 2001.